J Wood Sci (2011) 57:387–394
DOI 10.1007/s10086-011-1186-x

ORIGINAL ARTICLE

Sangdae Lee · Sang-Joon Lee · Jong Su Lee · Ki-Bok Kim
Jun-Jae Lee · Hwanmeyong Yeo

Basic study on nondestructive evaluation of artificial deterioration of a wooden rafter by ultrasonic measurement

Received: November 15, 2010 / Accepted: February 25, 2011 / Published online: June 28, 2011

Abstract Most old buildings in Korea are wood framed and, with age, deterioration is found in all wood components of antique buildings. Insects and rapid changes in humidity are among the main causes of deterioration. To preserve antique wooden buildings, nondestructive testing (NDT) methods are required. Various methods of nondestructive evaluation (NDE) such as X-ray, stress wave, drilling resistance test, and ultrasound are used to inspect the safety of wooden antique buildings. The ultrasonic method is relatively simple, inexpensive, and accurate. The rafters are one of the main components of antique buildings and are seriously affected by deterioration. This study aimed to develop a nondestructive ultrasonic technique for evaluation of wooden rafter deterioration. Regression models describing the relationship between the artificial deterioration of the specimen and ultrasonic parameters were proposed. The method was found to be reliable for evaluating wooden rafter deterioration.

Key words Nondestructive evaluation (NDE) · Rafter · Ultrasonic technique · Deterioration · Old wooden buildings

S. Lee · K.-B. Kim (✉)
Center for Safety Measurement, Korea Research Institute of Standards and Science, 1 Doryong-Dong, Yuseong-Gu, Daejeon 305-340, Korea
Tel. +82-42-868-5278; Fax +82-42-868-5650
e-mail: kimkibok@kriss.re.kr

S.-J. Lee
Department of Forest Sciences, Seoul National University, Seoul 151-921, Korea

J.S. Lee
Department of Gas Engineering, Kundong University, Andong 760-833, Korea

J.-J. Lee · H. Yeo
Department of Forest Sciences, Seoul National University, Seoul 151-921, Korea

Introduction

Most old buildings in Korea are wood framed. Components in these buildings that have been damaged by such agents as fungi and insects are often unable to support loads and need replacement. However, because most safety evaluations of a wooden structure consist of external inspections by the unaided eye, it is very difficult to determine internal conditions such as strength and degree of deterioration. Underestimating or overestimating the safety of wooden structural members can compromise their safety or lead to unnecessary costly repair work; neither alternative is desirable for older historic structures. The rafter, one of the main components of wooden buildings, supports the roof. Because more than half of the rafter is covered by the roof, deterioration of a rafter cannot be detected easily.

A nondestructive testing (NDT) method to evaluate the deterioration of the rafter covered by the roof is required. Various NDT methods for wooden structures include X-ray, stress wave, drilling resistance test, and ultrasound.[1,2] Among these, the nondestructive ultrasonic method has the merits of lower power consumption, lower cost, higher resolution, more applicability for various test materials, and simple design compared with other NDT methods. The propagation phenomena of ultrasound in wood differ from those in other materials because of the inhomogeneous, anisotropic, porous, and hygroscopic properties of wood. The main factor affecting the propagation of ultrasound in wood is its anisotropic property. Ultrasonic wave velocities in the longitudinal direction (along the fibers of wood), and in the radial and tangential directions in an annual ring of the wood, are different. Some differences in ultrasonic wave velocity were found to depend on the species of wood.[3–7] Ultrasonic waves are attenuated when propagating in the fiber direction of wood and in tangential and radial directions to an annual ring.[8] Ultrasonic wave velocity changes according to the change of moisture content of the wood[9] but is not affected by wood temperature.[10] Ultrasonic wave velocity increases, and transmitting ultrasonic energy decreases, with increase in frequency of ultrasonic waves in

wood.[6,8,11] Thus, detection of internal defects of wood using ultrasonic wave velocity is possible.[12,13] Other research results showed that ultrasonic energy was more effective than ultrasonic wave velocity for detecting internal defects of wood.[14–16]

In use, wooden rafters are often attacked by various environmental conditions. The most important agents of wood deterioration include fungi and insects. Toughness and weight loss have been considered to be the most sensitive indicators of the degree of wood deterioration caused by decay.[17,18] Especially, large holes have been found in secondary walls of wood.[19,20] In view of the changes shown in Fig. 1, this study chose to focus on weight loss and load at rupture as the parameters indicating wood decay.

In this study, ultrasonic parameters such as amplitude and magnitude areas obtained from time and frequency domains, respectively, were analyzed to evaluate deterioration of a wooden rafter nondestructively. Evaluation models for deterioration of a wooden rafter using the ultrasonic parameters defined in this study were presented.

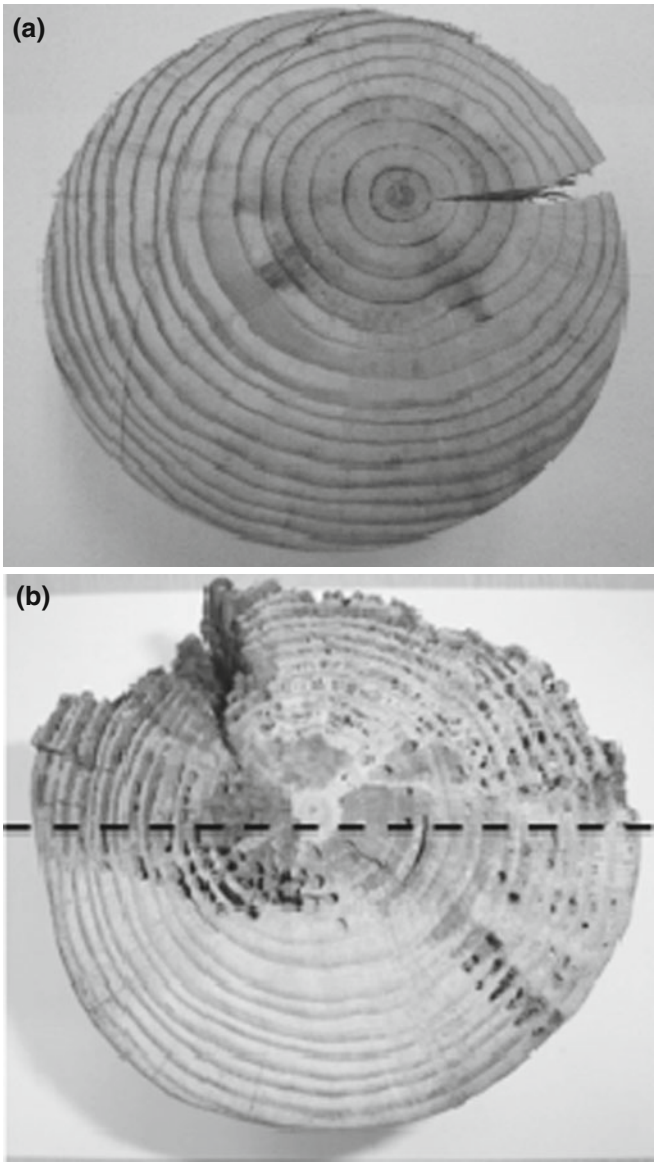

Fig. 1. Photographs of sound and unsound rafters. **a** Sound rafter. **b** Rafter rendered unsound by deterioration

Materials and methods

Principle

Ultrasonic testing generally uses through-transmission and pulse-echo techniques. However, it is very hard to apply general ultrasonic testing techniques to detect deterioration that occurs in the internal part of the rafter because it is partly covered by the roof. For ultrasonic testing of the rafter, a one-side testing technique was used (Fig. 2). An ultrasonic pulser and receiver are set in a row (Fig. 2a), and the ultrasonic wave generated by the ultrasonic pulser is sent through the surface and the inner part of the rafter to the ultrasonic receiver. For verification, a specimen 100 mm in diameter and 700 mm in length was fabricated and sawn 50 mm deep at its center to separate the ultrasonic signals transmitted through the surface and the inner part of the specimen. Figure 2a shows an ultrasonic signal transmitted through the whole specimen; Fig. 2b shows an ultrasonic signal transmitted through the inner part of the specimen. The TOF (time of flight) of the ultrasonic signal in Fig. 2b was increased because the ultrasonic signal was transmitted through the inner part of the specimen and not the surface, which is the shortest path. Amplitude was decreased under the half of the ultrasonic signal in Fig. 2a because it was not receiving the ultrasonic signal that was transmitted through the surface of the specimen. Figure 2c shows an ultrasonic signal transmitted through the surface of the specimen; TOF of the ultrasonic signal in Fig. 2c was the same in Fig. 2a. However, the amplitude of the received ultrasonic signal was decreased more than that in Fig. 2b because the ultrasonic signal, which was transmitted through the inner part of the specimen, was not received.

If the inner deterioration of the wooden rafter increases, the inner part in which the energy of the ultrasonic wave can be transmitted is decreased (Fig. 1b) and the energy of the ultrasonic signal received is ultimately decreased.[21] Therefore, deterioration of the wooden rafter can be evaluated by measuring the energy change of the received ultrasonic signal that is transmitted through it.

Specimen

A section of larch (*Larix leptolepis*) was fabricated into a test specimen 100 mm in diameter and 700 mm in length. Larch timbers of this size and shape are widely used as rafters in antique Korean wooden buildings. Air-dry specific gravity and moisture content of the specimen were 0.52 ± 0.01 and 14.2% ± 1.0%, respectively.

Because it was very difficult to create real deteriorated specimens with known conditions, test specimens were constructed of similar shape to a real wooden rafter. Because more than one-half of each wooden rafter is covered by the

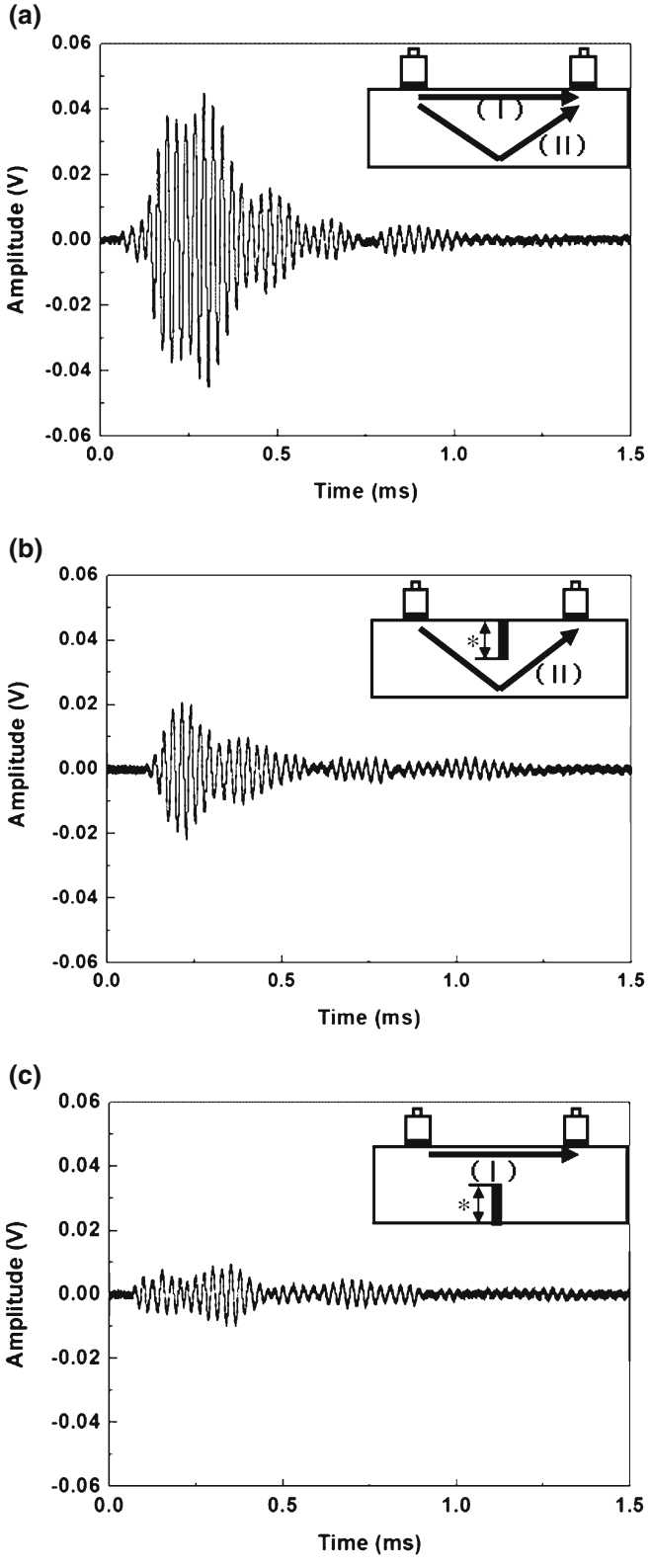

Fig. 2. Received ultrasonic signals and method of evaluating deterioration of the wooden rafter by one-side testing technique. **a** Whole specimen. **b** Inner part of the specimen. **c** Surface of the specimen. *Asterisk* 50 mm

roof, most deterioration occurs in that portion. To create a specimen of artificial deterioration, holes 8 mm in diameter were drilled normal to the axis at 15 mm intervals along its length. Five kinds of artificially deteriorated specimens were prepared, with drill-hole depths of 0, 20, 40, 60, and 80 mm, respectively. Three specimens were made for each drill-hole depth, a total of 15 specimens. As a deterioration parameter, the weight of specimens without and with drill-holes was calculated. Figure 3 shows the configuration of the specimen with drill-holes. Table 1 shows the weight loss of the specimen for each depth of drill-hole.

Ultrasonic measurement setup and method

Figure 4 shows the overall experimental setup consisting of the ultrasonic transducers and their holder, the specimen, ultrasonic pulser and receiver, oscilloscope, and personal computer. An ultrasonic transducer was fabricated with a curved wear plate (front matching layer) to create direct contact to the surface of a circular specimen and to effectively transmit and receive the ultrasonic wave. The central frequency and diameter of the ultrasonic transducer were 100 kHz and 40 mm, respectively. The fabricated ultrasonic transducer for wood mainly consisted of piezoelectric material (PZT), front matching layer, and back acoustic material. The front matching layer is made of Teflon to match the acoustic impedances between piezoelectric material and the specimen. Vacuum grease was used to transmit ultrasonic energy into the specimen without energy loss between the ultrasonic transducers and the specimen. A rod with an aluminum holder supported the transmitting and receiving ultrasonic transducers (Fig. 5). The distance between the two ultrasonic transducers was controllable. The transmitting ultrasonic transducer was fixed, and the receiving ultrasonic transducer was movable along the length of the specimen. All received ultrasonic signals were obtained at a 400 mm distance between transmitting and receiving transducers. To keep a uniform contacting pressure between each transducer and the specimen, springs with 40 mm in diameter and 50 mm in length were installed inside the holders. A high-power pulser/receiver (ARIMAX, USA) generated and received the ultrasonic wave. The ultrasonic wave signal that had passed through the specimen was acquired by the ultrasonic receiver, displayed on an oscilloscope, and analyzed in a personal computer.

Changes of the ultrasonic energy of the ultrasonic signal received through the specimen were analyzed to evaluate the degree of specimen deterioration. As evaluation parameters, considering the ultrasonic energy, two areas of received signals in time and frequency domains were defined by Eqs. 1 and 2 as

$$T_{\mathrm{A}} = \int_{t_1}^{t_2} |v(t)| dt \tag{1}$$

where T_{A} is amplitude area in time domain, $v(t)$ is amplitude (V), and t_1 and t_2 are times (s).

$$F_{\mathrm{A}} = \int_{f_2}^{f_1} |M(f)| df \tag{2}$$

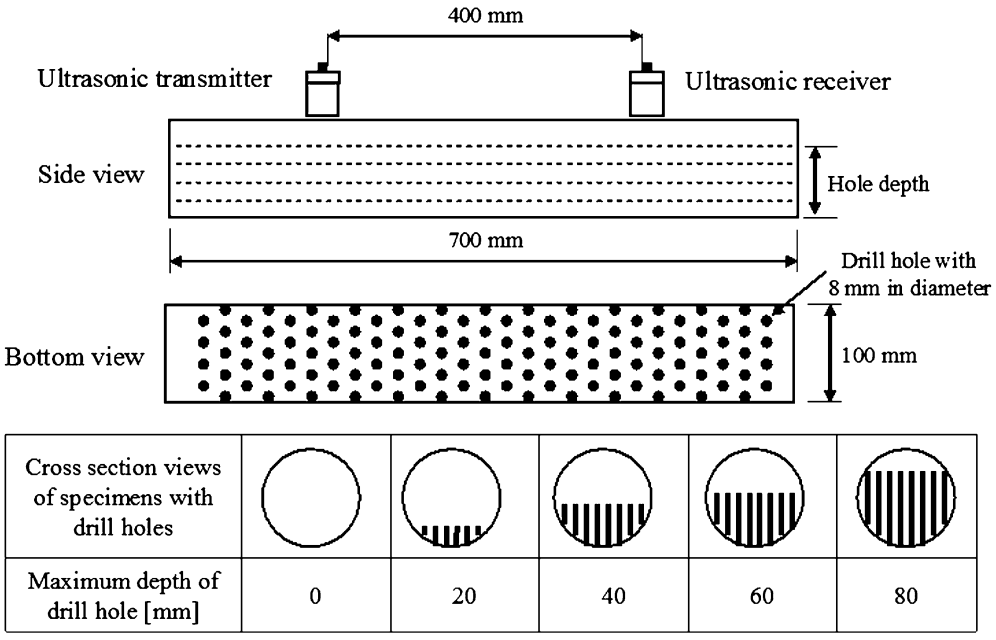

Fig. 3. Configuration of the specimen with drill-holes

Table 1. Weight loss of the specimen at each depth of drill-hole

Depth of drill-hole (mm)	Weight loss (%)		
	Specimen no. 1	Specimen no. 2	Specimen no. 3
0	0	0	0
20	7.24	8.16	9.21
40	12.26	12.80	13.69
60	22.20	21.98	22.09
80	27.15	29.13	29.05

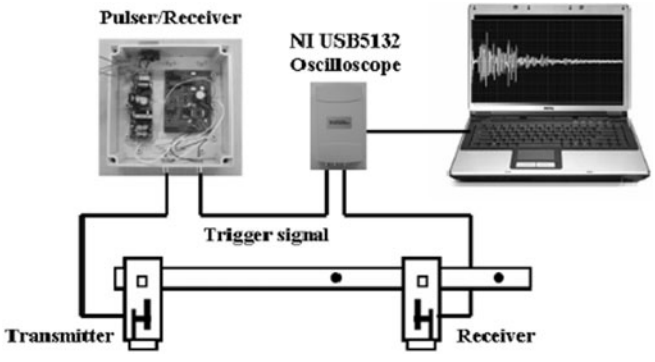

Fig. 4. Ultrasonic measurement setup

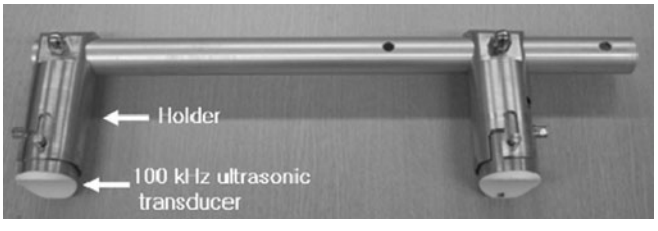

Fig. 5. Supporting rod with holder for ultrasonic transmitting and receiving transducers

where F_A is magnitude area in frequency domain, $M(f)$ is magnitude, and f_1 and f_2 are frequencies (Hz).

LabView software (Version 8.1; NI Inc., USA) was used to process the received ultrasonic wave signal. Figure 6 demonstrates the flow diagram of signal processing. The received ultrasonic wave signal in Fig. 6a was transformed by the fast Fourier transform (FFT) algorithm (Fig. 6b). The magnitude area in frequency domain (F_A) was calculated in the range of 20–60 kHz in Fig. 6b using Eq. 2. The frequency components below 5 kHz were eliminated with the high-pass filter because signal components below 5 kHz may be a noise source when calculating the amplitude area in time domain (T_A). The high-pass filtered signal was inverted by the inverse FFT algorithm (IFFT) (Fig. 6c). The envelope algorithm was applied to the high-pass filtered signal (Fig. 6d); the amplitude area in time domain was calculated as 0.1–1.5 ms.

Material test for compression perpendicular to grain

After the ultrasonic experiments, a compression test was conducted to measure the loading force at rupture using a universal testing machine (UTM). The modulus of rupture reflects the maximum load carrying in bending and is proportional to the maximum moment borne by the specimen.[22] The modulus of rupture is usually in load per unit cross-sectional area, load divided by the area without drilled holes minus the area of the drilled holes. In this study, because it was not easy to measure the exact area of the drilled holes, the rupture point, which represents load in Newtons at rupture, was used as the deterioration parameters. The loading rate of the crosshead was fixed at 5 mm/min for all test procedures. As compression progressed, a load–deformation curve was plotted automatically in relationship to the response of each specimen to the rupture

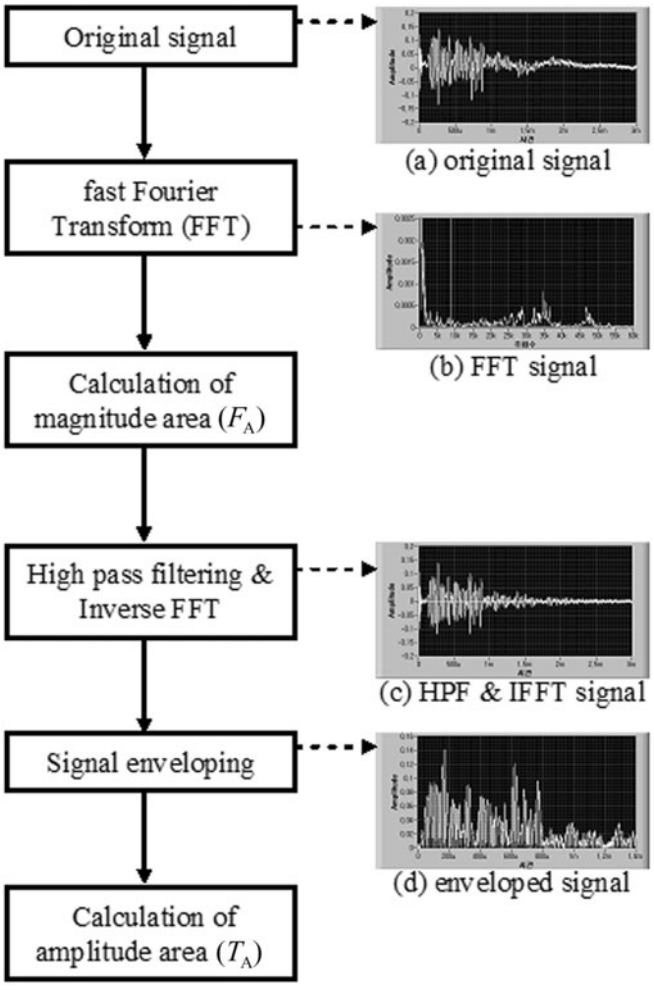

Fig. 6. Flow diagram of signal processing for calculating the amplitude and magnitude areas in time and frequency domains

point caused by compression. The rupture point was obtained from the load–deformation curve. All ultrasonic measurement and compression tests were conducted under room temperature (21° ± 1°C) and humidity (48% ± 3%) conditions.

Results and discussion

Progressive changes in the waveform of the received ultrasonic signal and the rupture point were caused by weight loss of the specimen. Changes in waveform of the received ultrasonic signal at weight loss from 0% to 22.20% are shown in Fig. 7, which shows ultrasonic signals originally obtained through the specimens, maximum amplitudes, and signal durations of the received signal that decreased as weight loss increased. Figure 7 indicates that the waveform and amplitude of the received ultrasonic signals are mainly dependent on the degree of artificial deterioration (depth of drill-hole), although the signals transmitted along the surface of the specimen are included.

The effect of deterioration on the rupture point of specimens (Fig. 8) indicates the change in rupture point decreased with as weight loss increased. The measured to rupture point of the specimen by the UTM decreased from about 20 kN (without weight loss) to about 3 kN (weight loss about 29%). The measured rupture point of the specimen without weight loss was more than six times that of the maximum weight loss. The measured rupture point of the specimen (Fig. 9) decreased with the weight loss from a very hard specimen (without weight loss) to a very soft specimen (weight loss about 29%).

Relationships were analyzed between ultrasonic parameters, such as amplitude area in time domain and magnitude area in frequency domain, and deterioration parameters, such as weight loss and rupture point of the specimen (Figs. 9, 10). Changes of amplitude area and magnitude area in time and frequency domains, respectively, of the received ultrasonic signals caused by weight loss of the specimen are shown in Fig. 9. The amplitude and magnitude areas decreased linearly with the increase of the weight loss of the specimen. Figure 10 shows a logarithmic relationship between amplitude and magnitude areas and the rupture point; amplitude and magnitude areas increased logarithmically with increase of weight loss of the specimen. Correlation analysis was performed on the relationships between ultrasonic parameters and deterioration parameters. Because amplitude and magnitude areas decrease linearly with weight loss, the following linear regression model was assumed:

$$y = ax + b \tag{3}$$

where y is amplitude area (T_A) or magnitude area (F_A) in time and frequency domains of the received ultrasonic signal, x is the weight loss of the specimen, and a and b are coefficients specific to each regression.

From Fig. 10, because the amplitude and magnitude areas increase logarithmically with increase of the rupture point, the following regression model based on logarithmic function was assumed:

$$y = a\ln(x) + b \tag{4}$$

where x is the rupture point of the specimen.

The statistical regression analysis results are summarized in Table 2. The amplitude area in time domain and magnitude area in frequency domain of the received ultrasonic signal defined in Eqs. 3 and 4 are highly significant parameters relating the deterioration of the specimen (weight loss and rupture point) with a correlation coefficient greater than 0.93.

The correlation coefficients (R) for Eq. 3 between the weight loss of the specimen and amplitude and magnitude areas were –0.988 and –0.983, respectively. The correlation coefficients for Eq. 4 between rupture point of the specimen and amplitude and magnitude areas were 0.964 and 0.938, respectively. The correlations between ultrasonic parameters and weight loss and rupture point suggest it is possible to predict deterioration of a wooden rafter by measuring its ultrasonic parameters.

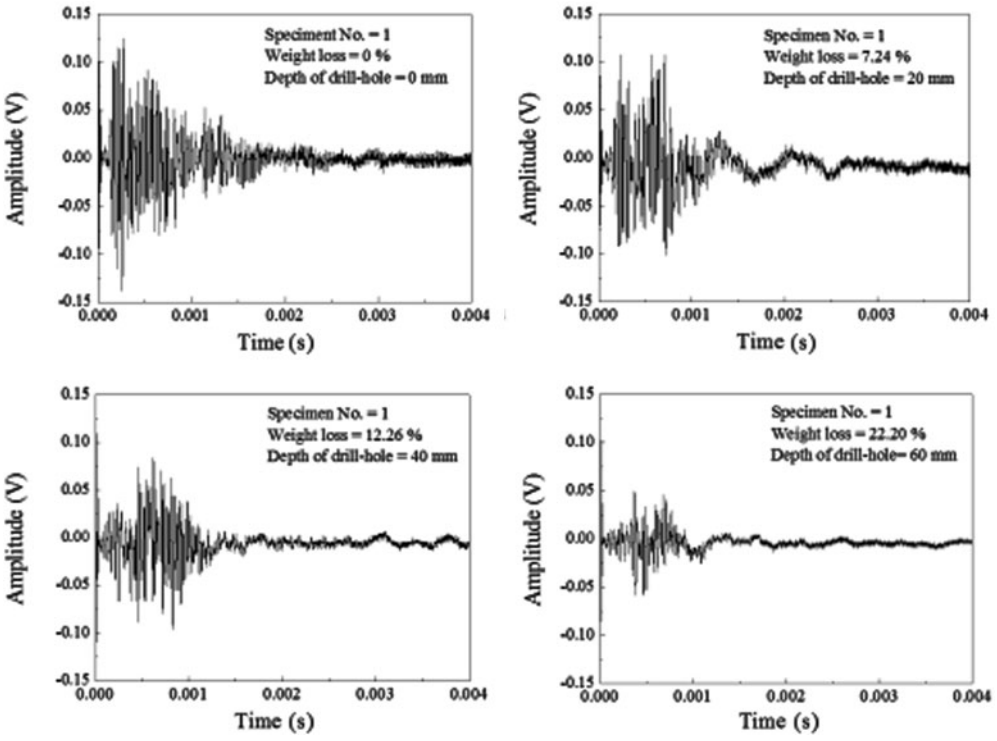

Fig. 7. Changes in ultrasonic signals in specimens measured at different stages of weight loss

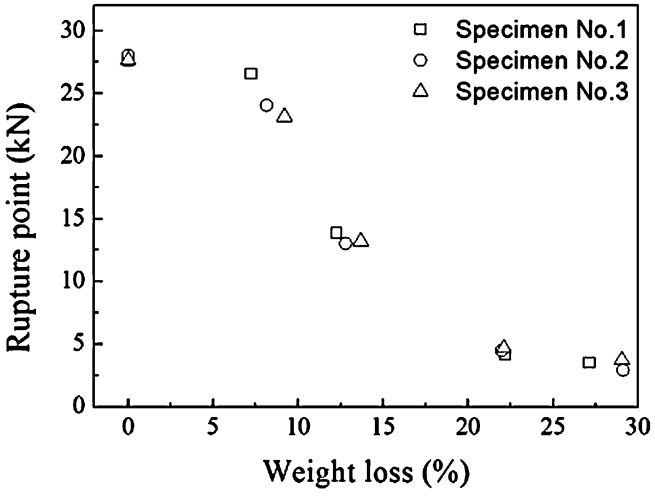

Fig. 8. Variation in mean value of rupture point (*kN*) with change of weight loss of specimen. **a** Amplitude area in time domain (T_A). **b** Magnitude area in frequency domain (F_A)

From Figs. 9 and 10, because the changes in the ultrasonic parameters (amplitude area and magnitude area) were dependent on the artificial deterioration parameters (weight loss and rupture point), determination of the deterioration of a wooden rafter using ultrasonic parameters seemed possible.

To estimate capability of determining weight loss and rupture point with amplitude and magnitude areas, two regression models were assumed:

$$\mathrm{WL} = aT_{\mathrm{A}} + bF_{\mathrm{A}} + c \tag{5}$$

$$\ln(\mathrm{RP}) = aT_{\mathrm{A}} + bF_{\mathrm{A}} + c \tag{6}$$

where WL is weight loss (%), RP is rupture point (kN), and a, b, and c are regression coefficients.

Equation 5 describes the linear relationships between weight loss and ultrasonic parameters, and Eq. 6 describes the logarithmic relationship between the rupture point and ultrasonic parameters, respectively.

Figures 11 and 12 show predicted versus measured values of the artificial deterioration factors and demonstrate the feasibility of the ultrasonic technique for estimating wooden rafter deterioration. Statistical regression analysis results are summarized in Table 3. Coefficients of determination (R^2) of regression models for weight loss and rupture point are 0.969 and 0.920, respectively. The regression analysis suggested deterioration of a wooden rafter will be predictable using ultrasonic measurement. The calibration equations for artificial deterioration of wooden rafters were based on the results seen in Table 3. The developed calibration equations were then used to predict artificial deterioration using measured ultrasonic parameters.

Conclusions

This study was performed to evaluate deterioration of a wooden rafter using a nondestructive ultrasonic technique. As the deterioration factors, weight loss and rupture point of specimens with drill holes were measured. To consider the ultrasonic energies propagating into the specimen, amplitude and magnitude areas of ultrasonic signal received through the specimen in time and frequency domains were calculated. Progressive changes occurred in the waveform

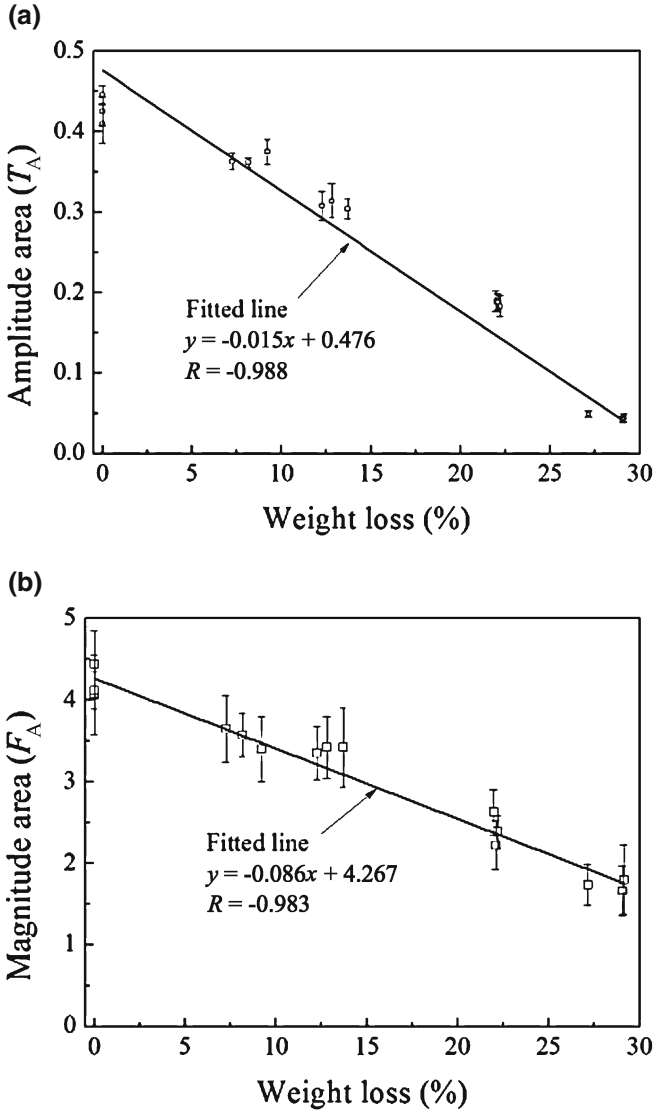

Fig. 9. Variation of mean values of amplitude area in time domain (**a**) and magnitude area in frequency domain (**b**) with weight loss of specimen. *Vertical lines*, confidence intervals: level of confidence is 95%

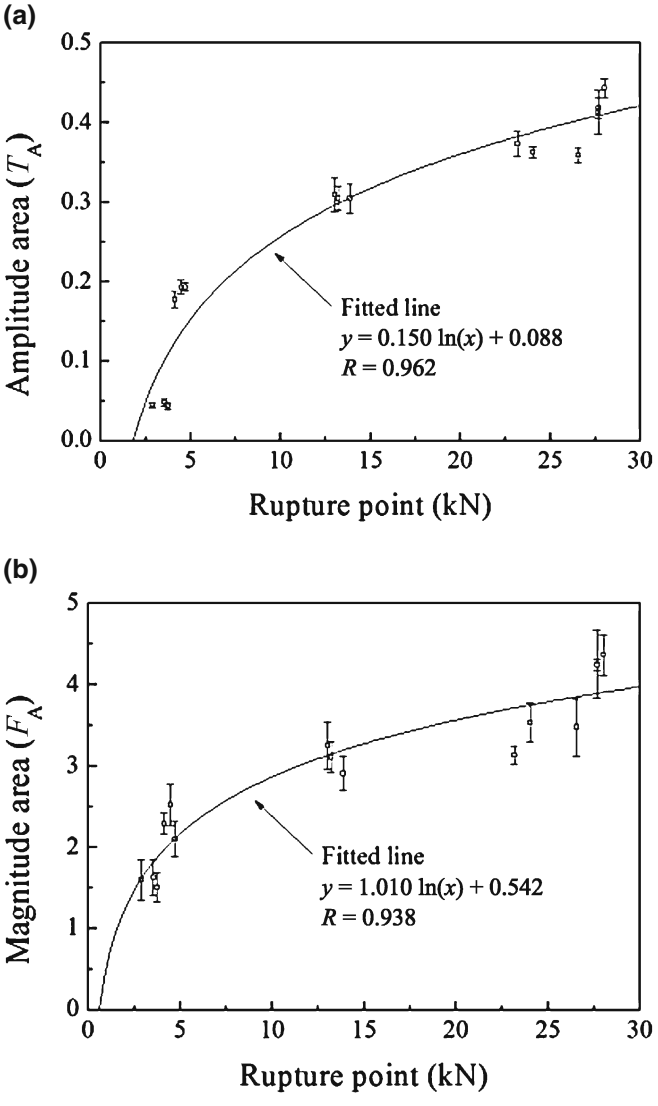

Fig. 10. Variation of the mean values of amplitude area in time domain (**a**) and magnitude area in frequency domain (**b**) with rupture point of specimen. *Vertical lines*, confidence intervals: level of confidence is 95%

of ultrasonic signal received and the rupture point caused by the change of specimen weight. Amplitude area and magnitude area of received ultrasonic signal decreased linearly with the increase of weight loss of the specimen but increased logarithmically with the increase of rupture point of the specimen. The correlation coefficients for the linear relationship between weight loss of the specimen and the amplitude and magnitude areas were 0.988 and 0.983, respectively. Correlation coefficients for the logarithmic relationship between the rupture point of the specimen and amplitude and magnitude areas were 0.964 and 0.938, respectively. Two regression models describing the relationship between the artificial deterioration of the specimen and ultrasonic parameters were proposed, and the method was found to be reliable for predicting the deterioration of a wooden rafter. The technique for predicting the artificial deterioration of a wooden rafter based on ultrasonic parameters may provide a promising method for the realization of nondestructive practical instruments in measuring deterioration of the components of wooden buildings.

Table 2. Correlation coefficients for ultrasonic parameters versus deterioration parameters regressions

Model	Independent variable	Dependent variable	Correlation coefficient
$y = ax + b$	Weight loss	Amplitude area, T_A	–0.988
		Magnitude area, F_A	–0.983
$y = a\ln(x) + b$	Rupture point	Amplitude area, T_A	0.964
		Magnitude area, F_A	0.938

Acknowledgments This work was supported by the Korea Science and Engineering Foundation (KOSEF) grant funded by the Korea government (MOEST). The authors also thank Professor David K. Hsu of the Center for NDE, Iowa State University, for some useful suggestions.

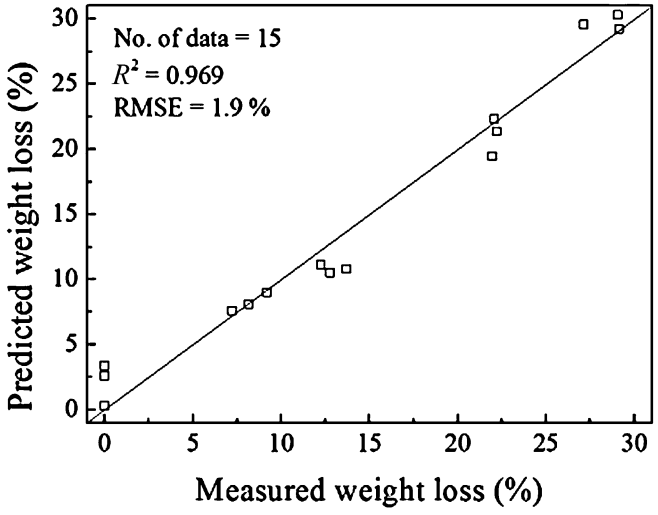

Fig. 11. Relationship between change of volume (% weight loss) by measurement and as predicted by Eq. 5. *RMSE*, root mean square error

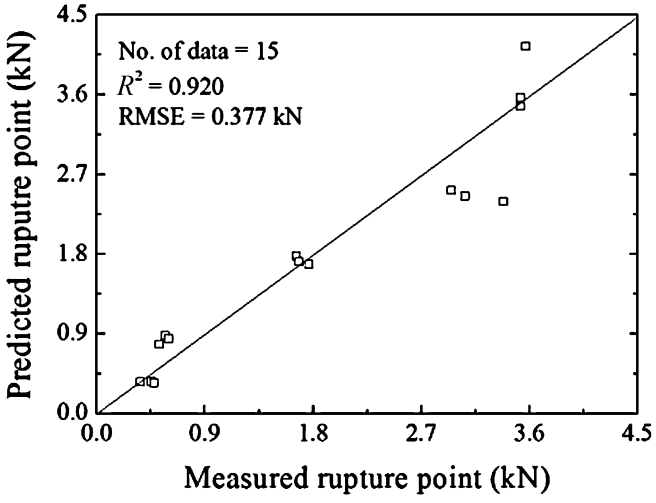

Fig. 12. Relationship between measured rupture point by universal testing machine (UTM) and rupture point predicted by Eq. 6

Table 3. Results of regression analysis for deterioration as a function of ultrasonic parameters

Model	Regression coefficients			Coefficient of determination (R^2)	Root mean square error (RMSE)
	a	*b*	*c*		
$WL = aT_A + bF_A + c$	–27.992	–6.915	42.949	0.969	1.9%
$\ln(RP) = aT_A + bF_A + c$	5.603	0.086	0.622	0.920	0.377 kN

References

1. Lee SJ, Kim KM, Lee JJ (2006) Application of the X-ray CT technique for NDE of wood in field. Key Eng Mater 321-323:1172–1176
2. Rui F, Lihong Q, Huawei C, Akio O, Hiroshi U, Katsuhiko S (2009) Application of a drill resistance technique for rapid determining wood density. Key Eng Mater 407-408:494–499
3. Gerhards CC (1980) Effect of cross grain on stress waves in lumber. RP-FPL-RP-368. Forest Product Laboratory, U.S. Department of Agriculture Forest Service, Madison, WI
4. Bucur V (1998) Wood structural anisotropy estimated by acoustic invariants. IAWA Bull 9:67–74
5. Armstrong JP, Patterson DW, Sneckenberger JE (1991) Comparison of three equations for predicting stress wave velocity as a function of grain angle. Wood Fiber Sci 23:32–43
6. Bucur V, Feeney F (1992) Attenuation of ultrasound in solid wood. Ultrasonics 30(2):76–81
7. Kabir MF (2001) Prediction of ultrasonic properties from grain angle. J Inst Wood Sci 15:235–246
8. Bucur V, Böhnke I (1994) Factors affecting ultrasonic measurements in solid wood. Ultrasonics 32:385–390
9. Gerhards CC (1982) Longitudinal stress waves for lumber stress grading: factors affecting applications: state of the art. For Prod J 32:20–25
10. Kang H, Booker RE (2002) Variation of stress wave velocity with MC and temperature. Wood Sci Technol 36:41–54
11. Niemz P, Kucera J, Schob M, Scheffer M (1999) Possibility of defect detection in wood with ultrasound. Holz Als Roh- Werkstoff 57(2):96–102
12. Wilcox WW (1988) Detection of early stages of wood decay with ultrasonic pulse velocity. For Prod J 38:68–73
13. Han W, Birkeland R (1992) Log scanning through combination of ultrasonics and artificial intelligence. In: Proceedings, 8th International Symposium on Nondestructive Testing of Wood, Vancouver, WA, pp 163–187
14. Brashaw BK, Adams RR, Schafer ME, Ross RJ, Pattersen RC (2000) Detection of wet wood in green red oak lumber by ultrasound and gas chromatography-mass spectrometry analysis. In: Proceedings, 12th International Symposium on Nondestructive Testing of Wood, Sopron, Hungary, pp 49–56
15. Ross RJ, DeGroot RC, Nelson WJ, Lebow PK (1997) The relationship between stress wave transmission characteristics and the compressive strength of biologically degraded wood. For Prod J 47: 89–93
16. Ross RJ, Pellerin RF, Forsoman JF, Erickson JR, Lavinder JA (2001) Relationship between stress wave transmission time and compressive properties of timber removed from service. FPL-RN-280. Forest Products Laboratory, U.S. Department of Agriculture Forest Service, Madison, WI
17. Hennon P, Woodward B, Lebow P (2007) Deterioration of wood from live and dead Alaska yellow-cedar in contact with soil. For Prod J 57:23–30
18. Morrell JJ, Zabel RA (1985) Wood strength and weight loss caused by soft-rot fungi isolated from treated southern pine utility poles. Wood Fiber Sci 17:132–143
19. Blanchette RA, Nilsson T, Daniel G, Abad A (1990) Biological degradation of wood. In: Rowel RM, Barbour FJ (eds) Archaeological wood: properties, chemistry, and preservation. American Chemical Society, Washington. DC. Adv Chem Ser 225:141–174
20. Eaton RA, Hale MDC (1993) Wood: decay pests and protection. Chapman & Hall, London
21. Sandoz JL, Benoit Y, Demay L (2000) Wood testing using acousto-ultrasonic technique. In: Proceedings, 12th International Symposium on Nondestructive Testing of Wood, University of Western Hungary, Sopron, pp 97–104
22. Green DW (2001) Wood: strength and stiffness. In: Encyclopedia of materials: science and technology. Elsevier, Amsterdam, pp 9732–9736